Materials Today: Proceedings xxx (xxxx) xxx

Contents lists available at ScienceDirect

Materials Today: Proceedings

journal homepage: www.elsevier.com/locate/matpr

Biobased composite powders from PHA, waxes and lignocellulosic biomasses for powder-based additive manufacturing processes

Claire Mayer-Laigle [a,b,*], Christophe Collet [b], Yi Chen [b], Mark West [b], Rob Whitton [b], Marie-Joo Le Guen [b]

[a] IATE, Université de Montpellier, INRAE, Institut Agro-Montpellier SupAgro, 34060 Montpellier, France
[b] Scion, 49 Sala Street, Rotorua 3010, New Zealand

ARTICLE INFO

Article history:
Available online xxxx

Keywords:
Additive manufacturing
Selective laser sintering
Biobased materials
Polyhydroxyalkanoate
Waxes
Biocomposite powder

ABSTRACT

Reducing our impact on the environment requires the use of biobased materials and their composites, which can be sourced from biomass feedstocks. However, due to technological limitations, these materials are not easily integrated into current Additive Manufacturing technologies like Selective Laser Sintering.

The focus of the present study is to develop a new, environmentally friendly process that can prepare composite biobased powders for SLS. These powders are made from polyhydroxyalkanoate, waxes, and lignocellulosic fillers. The process is based on emulsification and dissolution/precipitation in eutectic solvents and has the potential to be utilized with a wide range of biobased materials.

1. Introduction

Additive manufacturing (AM) is a layer-by-layer production method that reduces the amount of raw material needed in comparison to subtractive techniques. The societal shift towards a circular bioeconomy has prompted efforts to combine AM with environmentally sustainable materials. Saidani et al, proposed a classification system that considers a comprehensive range of biobased material alternatives based on their biodegradability and the environmental impact of their production processes (CO_2 equivalent) [1]. Among these materials, polyhydroxyalkanoates (PHAs), which are microbial biopolymers, was suggested as a promising material due to their excellent biocompatibility and biodegradability [2]. However, their weak mechanical strength, hydrophilicity and low crystallization rate [3], complicates their use in traditional 3D printing processes [4]. Numerous studies have investigated the use of lignocellulosic powders as functional reinforcing fillers to increase the crystallisation rate and the mechanical properties of PHAs [5–8]. Natural waxes (e.g. beeswaxes and vegetable waxes) are also biocompatible and biodegradable, and possess hydrophobic and antibacterial properties [9]. It has been shown that the addition of crystalline waxes can improve the crystallisation process for low-density polyethylene [10] and reduce the setting time of hot melt adhesive [11,12]. Waxes have also been used to tune the properties of PHA/wheat bran composite as a compatibiliser between the lignocellulosic filler and polymeric matrix [13]. Thus, by formulating PHA with biobased waxes and lignocellulosic biomass, the properties of PHA can be enhanced, enabling the design of biobased, biodegradable, and biocompatible materials with improved mechanical, hydrophobicity and antibacterial properties, depending on the specific formulation used.

However, the rheological and mechanical properties of such composites make it challenging to produce filaments for Fused Deposition Modelling (FDM) techniques, one on the most common AM techniques used for biobased materials. [14]. Paste deposition processes can be employed but the resolution of complex objects remains weak [15]. Instead, selective laser sintering (SLS) is a more promising AM technique for such materials. SLS is a powder bed fusion-based additive manufacturing technology that uses a laser system to form objects by sintering powdered materials layer by layer. Compared to other AM techniques, SLS has many advantages such as high accuracy, speed, reliability and lack of support structures, and it is a robust commercial AM technology. Initially, SLS was used for the additive manufacturing of metals, and currently, the range of commercially available powdered polymer materials that can be used in the process is limited. Polyamide (PA) is the

* Corresponding author at: IATE, Université de Montpellier, INRAE, Institut Agro-Montpellier SupAgro, 34060 Montpellier, France.
E-mail address: claire.mayer@inrae.fr (C. Mayer-Laigle).

https://doi.org/10.1016/j.matpr.2023.05.052

most widely used commercial material [16]. Over the past two years, there has been increasing interest in the development of new biodegradable and biobased polymer and composite powders, with potential applications in advanced fields such as pharmaceuticals and tissue engineering [16–18] for which a formulation from PHA/Waxes/biobased filler would be attractive.

The quality of 3D printed objects produced using SLS is directly related to the microstructure of the powder bed depending on intrinsic and bulk properties of the powders [16,19–21]. The particle size distribution of the powder, in particular the median particle size and dispersion of the distribution, is crucial, as it directly influences the spreadability of the powder in the SLS printer (quantification of the ease with which a powder is spread uniformly), the dimensional accuracy and the porosity of the 3D printed object. Obtaining fine and easily spreadable biobased composite powders is challenging. Typically, when printing such polymers by SLS, blends of powders from different materials are used [22,23], but composite particles are better suited to the SLS process as it reduces segregation between the different compounds of the blend and enables better interaction between filler and matrix. Milling of composites obtained from compounding generates a broad particle size dispersion that reduces the spreadability of the powder. Additionally, milling is not suitable for matrices with low glass transition and melting temperatures, such as wax. Finally, from a green process perspective, the ideal situation for an AM process would be to use the PHA in the form of microspheres directly, as produced within the microorganism, rather than milling PHA granules to obtain a fine powder. Therefore, there is pressing need to develop new biobased composite formulations with improved properties compare to pure matrices, which can be suitable for SLS technologies.

Particles with a regular shape have been previously prepared from waxes by melt emulsification processes. In such processes, the dispersed phase is heated above its solidification temperature in a continuous phase with emulsifiers. High shear mixing is applied to disperse the emulsion into droplets. Then, the emulsion is rapidly cooled by adding cold water to solidify the droplets, and a suspension of spherical particles is obtained [24]. Alternatively, solid particles can be used as surfactant to stabilise the emulsion (i.e. Pickering emulsion) [25]. Composite wax particles prepared by emulsification from petroleum-based waxes have been reported [26,27]. In an original approach, by using water as emulsification solvent, this process could be extended to other biobased matrices which have a melting point below 90 °C.

For polymers with higher melting points, the use of dissolution-precipitation [18] or thermally induced phase separation processes (TIPS) [16] have been proposed to produce spherical particles suitable for SLS applications. These processes have been used to produce polyamide 12/carbon fibre (PA12/CF), neat polyether ether ketone (PEEK) and PEEK/carbon nanotubes (CNTs) composite powders. In the dissolution-precipitation process, polymer is dissolved in a suitable solvent, and filler is added to form a homogeneous suspension. The suspension is then gradually cooled to ambient temperature. The polymer crystallises, using the filler as heterogeneous nuclei. Finally, the composite powder is recovered after distilling out the solvent, vacuum drying and milling. In the TIPS process, polymer is dissolved in a solvent at elevated temperature followed by liquid–liquid phase separation (LLPS), droplet nucleation, and growth and precipitation during the subsequent cooling stage. In both cases, the solvents used are not green and the process requires steps for solvent recycling. However, in recent years, deep eutectic solvents (DES) as choline chloride (Ch-Cl), carboxylic acids, and other hydrogen-bond donors, e.g., urea, citric acid, succinic acid and glycerol appear to be an inexpensive and sustainable alternative to traditional solvents [28].

Using biobased materials for 3D printing, and more specifically for powder-based AM processes, is just emerging and there are currently no commercial composite biobased materials that can meet market expectations. In an innovative way, this work aimed to develop new and sustainable processes to produce composite particles for SLS printing by the combining of PHA, biobased waxes and lignocellulosic powder as a filler. Two processes have been proposed, to cover the whole range of the PHA family and their potential to generate particles suitable for SLS printing was evaluated by comparing their particle size distributions with that of PA12, a standard polymer powder for SLS printing.

2. Materials and methods

2.1. Raw materials

The raw materials included in the formulations were purchased/prepared as described below. The particle sizes and melting temperatures of the raw materials are reported in Table 1. Particle size distribution was measured by laser diffraction according to the protocol in section 3.5: Particle size analysis. Melting temperatures are provided in supplier datasheets (for the materials abbreviated PHB and BW) or measured experimentally by measuring the temperature of the solid/liquid transition (for the material abbreviated mcl-PHA).

Wax: Refined yellow beeswax pellets were purchased from NZ Beeswax Ltd. This is referred as beeswax in the remainder of the document, and abbreviated as BW.

PHA: Two types of PHA with different melting points were used: A fine powder of Poly[(R)-3-hydroxybutyric acid] (abbreviated PHB) purchased from Sigma-Aldrich (product 363502), and a medium-chain-length-Poly(3-hydroxyalkanoate) (abbreviated mcl-PHA) produced and purified according to the procedure described by Collet et al.[29] and Abbel and al. [30] respectively.

Lignocellulosic filler: The lignocellulosic powders used in this study are maritime pine bark (*Pinus pinaster*) purchased from a local store (Botanic, Montpellier, France) which was finely milled in three steps (coarse, intermediate and fine milling) with a vibratory ball mill according to the procedure described by Rajaonarivony et al. [31]. This powder is named pine bark powder (abbreviated PB) in the remainder of the document.

Choline-Chloride-Urea solvent: was prepared from choline chloride purchased from Sigma Aldrich (CAS Number 67–48-1) and urea purchased from Merck (CAS number 57–13-6) in the molar ratio 1:2. Before mixing, both compounds were oven-dried at 55 °C for 12 h [32]. The dried powders were then mixed at 80 °C until completely melted to produce the solvent, which was stored in an oven at 55 °C to prevent water uptake. The solvent is abbreviated to Ch-Cl-Ur.

2.2. Formulations

Different formulations (8 in total) were selected to screen a range of ratios and assess the potential of both processes in a limited number of trials (see Table 2). Raw material used in the formulation was tested alone and in combination. When lignocellulosic biomass was added as a filler, the mass proportion of the matrix (PHA, BW or PHA + BW) and those of the fillers were 60 wt% and 40 wt%, respectively.

2.3. Melt emulsification process

This process was applied to formulations 1 to 4. The matrix (mcl-PHA, or/and BW) and lignocellulosic powder (PB) were melted in a beaker on a hot-plate and mixed by magnetic stirrer.

Table 1
Particle size characteristics and melting temperature of the raw materials.

	Particle size characteristics				Melting temperature
	D_{10}	D_{50}	D_{90}	SPAN	
mcl-PHA	0.689	1.197	3.451	2.306	48.4 °C
PHB	3.9565	26.8135	74.827	2.643	172 °C
BW	Pellets (length: 2–4 cm, diameter 0.5 – 1 cm)				55 °C
PB	3.346	21.427	78.441	3.505	

Table 2
Description of the different formulations per weight fraction.

N°	Formulations	mcl-PHA (wt%)	PHB (wt%)	BW (wt%)	PB (wt%)
1	mcl-PHA-PB	60	–	–	40
2	mcl-PHA -BW-PB	20	–	40	40
3	BW	–	–	100	–
4	BW-PB	–	–	60	40
5	PHB	–	100	–	–
6	PHB-BW	–	50	50	–
7	PHB-PB	–	60	–	40
8	PHB-BW-PB	–	30	30	40

Hot water (90 °C) was then added to the mixture to create an oil-in-water emulsion. Different ratios o/w (oil in water) between 0.1 and 0.25 v/v (in volume) were tested in preliminary work and a ratio of 0.2 was selected for the results presented here as it leads to the more homogeneous emulsion.

The mixture was maintained at 90 °C and continuously homogenised for 5 min using a rotor/stator device (Ultra-Turrax T 25 disperser IKA® T25, Germany) operating at 12,500 rpm. Then, while maintaining the homogenisation, the emulsion was rapidly cooled by direct addition of ice until it dropped to temperature below 20 °C. This led to solidification of the droplets into particles, that were then separated from the liquid phase by filtration.

2.4. Dissolution and precipitation in Choline-Chloride

The different compounds (BW, PHB and PB) were first dissolved and/or melted in Ch-Cl-Ur for 12 h at 80 °C. Then, water (2 °C) was added. The simultaneous modification of the temperature and the ionic balance of the solution lead to the generation of particles. As the use of Ch-Cl-Ur to dissolve PHA and melt waxes has not yet been studied, two sets of experiments were carried out to understand the solubility of each compound of the matrix and their miscibility.

Set 1: For formulations 3 to 8, 500 mg of the raw materials were melted or dissolved in 15 ml of Ch-Cl-Ur for 12 h at 80 °C in the ratio reported in Table 2. Subsequently 2 ml of the solution was taken and 10 ml of water (2 °C) was added with stirring to precipitate the composite particles. The temperature of the final mixtures (including water) was below 12 °C. Two controls were carried out with pure Ch-Cl-Ur and Pure Pine bark powder (500 mg). In the first case, no precipitation was observed, and in the second case, the particle size distribution after 12 h at 80 °C was similar to that of the raw powder, suggesting no significant dissolution of pine bark powder in the solvent.

Set 2: To study the effect of dissolving/melting PHB and beeswax, two additional experiments were carried out as described below:

- 1 ml of the solution containing only PHB (Formulation 5. PHB) and 1 ml of the solution containing only the beeswax (Formulation 3. BW) were mixed just before the addition of 10 ml of cold water (2 °C) to generate composite particles (Formulation 6. PHB-BW)
- 0.6 ml of the solution containing only PHB (Formulation 5. PHB), 0.6 ml of the solution containing only the beeswax (Formulation 3. BW) and 0.8 ml of the control solution with only pine bark powder were mixed just before the addition of 10 ml of cold water to generate composite particles (Formulation 8. PHB-BW-PB)

2.5. Particle analyses

Microscopy: The images were captured using a Leica M125C stereomicroscope (Leica, Japan) and analysed using ImageJ software.

Particle size analysis: The particle size distributions of the composite powders were measured by laser diffraction using a Mastersizer 2000 (Malvern, UK) equipped with a Hydro2000S system. Data was processed using the Fraunhofer method [33]. Particle size distribution was recorded and main indicators, d_{10}, d_{50} d_{90}, SPAN ($(d_{90} - d_{10})/d_{50}$) and specific surface area, were extracted from the distribution. Measurements were carried out in triplicate and average particle size distribution was calculated.

2.6. Selective laser sintering of the powders

Selective Laser Sintering of the powders was carried out with a CO_2 laser machine (Makerspace G640L, New Zealand) with an adjustable laser power up to 75 W. Three formulations were tested namely: 1. ME.mcl-PHA-PB, 2. ME.mcl-PHA-BW-PB and 4. ME-BW-PB.

The powders were manually spread in a single powder layer on a dedicated support featuring 12 cavities with dimensions 30 mm × 30 mm and a depth of 0.75 mm, designed to hold the powder. The powders were sintered with a single laser pass operating at different levels of power in between 8% and 25% of the full power (75 W) at a moving speed of 30 mm/s at ambient conditions (23° C and 50% relative humidity (RH)).

3. Results and discussion

3.1. Melt emulsification process

Obtaining satisfactory melt emulsion required high shear mixing. The quick addition of ice was successful in generating particles. In the case of particles including the lignocellulosic biomass

as a filler (1. ME-mcl-PHA-PB, 2. ME-mcl-PHA-BW-PB, 4. ME-BW-PB) a rapid sedimentation of particles that were easily separated from the solvent by filtration was observed in the beaker. Sedimentation was not observed for Formulation 3. ME-BW due to a greater proportion of smaller particles, as illustrated in Table 3, summarising the main indicators of the particle size distribution (d_{50} = 1.8 μm).

Microscopic observations (Fig. 1) of the coarser particles of this formulation revealed spherical particles. The more angular appearance of composite particles from ME-BW-PB may be related to the coating of the beeswax droplets by the pine bark particles creating a Pickering emulsion and favouring the generation of larger particles.

Note that in the case of the three-component formulations that include pine bark powder as a filler, the median particle sizes were very close to those of PA12 (see Table 3). The value of SPAN, highlighting the scattering of the distribution is slightly broader than those of PA12 in relation to the lower and higher value of the 10th (d_{10}) and the 90th (d_{90}) percentiles of the distribution (giving an indication of the size of the smaller and larger particles). However, all the d_{90} values are below 150 μm and are still within the range of other commercial powders used in SLS processes [34].

3.2. Dissolution and precipitation in choline-chloride

Visual observations of Formulation 5.DP-PHB after dissolution did not detect any remaining particles, and the particle size indicators after the precipitation step (Table 3) are very different from those of raw PHB (Table 1), showing a successful dissolution of the polymer and then precipitation of the PHB in particles of smaller size. The span of the particle size distribution is larger than that of PA12, however a higher shear stirring system should result in more homogenous particle size distributions. The powder generated from the formulation with pure compounds (3. DP-BW, 5. DP-PHB) has a median particle size smaller than 10 μm that can lead to spreadability issues, prior to the printing process, or during the printing process itself. For the other formulations, the median particle sizes are typically in a range comparable to the commercial powder used for SLS printing. However, the d_{90} 8. DP-PHB-BW-PB (Set 1) is greater than 200 μm and so less suitable for SLS printing [35].

For formulations 6. DP-PHB-BW and 8. DP-PHB-BW-PB, the difference between the experiments carried out in

Set 1 and Set 2 is attributed to the duration in which the different components are in contact at 80 °C before precipitation (12 h in the case of Set 1, and approximatively 5 min in the case of Set 2). The high differences observed for the main indicators of the particle size distribution suggest stronger interactions between the compounds in the case of Set 1. These interactions could be due to polymer and wax interaction in the presence of Ch-Cl-Ur during the dissolution time. Deep eutectic solvents (DES) have been reported to induce structural change in the polymer structure [36]. Interestingly the particle size indicators obtained during the precipitation of the pure component (3 DP-BW, 5. DP-PHB and 6. DP-PHB-BW) indicated that the beeswax potentially triggers the formation of the particles in formulation 6. DP-PHB-BW as this particle size distribution is closer to those of 3. DP-BW than that of 5. DP-PHB.

3.3. Composite nature of the powders

To confirm the composite nature of the powders, i.e: the 3 compounds embedded in the same particle, the particle size distributions of powders precipitated separately (3-DP-BW, 5DP-PHB and pine bark powder), have been compared to those mixed after precipitation (8-PHB-BW-PB-blend) and to those of Formulation 8. DP-PHB-BW-PB Sets 1 and 2 (Fig. 2).

In Fig. 2a the particle size distribution of 8. PHB-BW-PB-blend is typically the mathematical sum of the particle size distribution of each powder alone. Conversely, the particle size distributions of 8. DP-PHB-BW-PB Set 1and Set 2 are shifting through coarser particles which is particularly significant for 8 DP-PHB-PB (Fig. 2b)., where the components remain a long time in contact before precipitation. This suggests that in the case of 8. DP PHB-BW-PB Sets 1 and 2, the particles are made of several components, and the contact time prior to the precipitation is crucial for managing the size and the properties of the composite particles. Further chemical analysis is planned in the coming months to investigate the nature of these interactions during the melting step, and their impact on the particles and powder properties in view of process optimisation.

3.4. Printability of the powder with selective laser sintering (SLS)

Simple printing tests were carried out with single line scan to determine the ability of the composite powders to be sintered. The tests were conducted at different power levels ranging from 8% to 25% of the full power (75 W) (Fig. 3). Visual assessment indicated that higher power resulting in increasing width of the bands, related to a melting of the powder rather than a sintering (i.e local melting at the surface of the particles). The resolution of the printing appears to be related to the compacity of the powder bed in close correlation to the particle size characteristics (d_{10}, d_{50}, d_{90} and Span). Thus, Formulation 4 (ME-mcl-PHA-PB), which appears

Table 3
Particle size characteristics and specific surface area of the different formulations.

	Formulation	d_{10} μm	d_{50} μm	d_{90} μm	Span $(d_{90} - d_{10})/d_{50}$	Specific surface area ($m^2.g^{-1}$)
	SLS reference powder					
	PA12	35.4	55.9	85.5	0.89	0.13
	Melt emulsification Processes (ME)					
	1. ME-mcl-PHA-PB	16.3	47.5	99.6	1.75	0.29
	2. ME-mcl-PHA-BW-PB	19.7	53.6	122	1.92	0.26
	3. ME-BW	0.8	1.8	43.4	24.2	3.61
	4. ME-BW-PB	22.5	72.5	145	1.69	0.21
	Dissolution/Precipitation in Choline-Chloride (DP)					
Set 1	3. DP-BW	1.61	7.55	32.5	3.91	1.34
	4. DP-BW-PB	22.2	54.7	102	1.46	0.25
	5. DP-PHB	1.64	6.40	32.3	4.77	1.63
	6. DP-PHB-BW	4.26	34.8	110	3.03	0.59
	7. DP-PHB-PB	2.64	12.7	47.5	3.55	0.99
	8. DP-PHB-BW-PB	7.35	78.8	327	4.04	0.37
Set 2	6. DP-PHB-BW	2.36	14.5	54.5	3.59	2.36
	8. DP-PHB-BW-PB	2.25	11.6	51.1	4.20	1.06

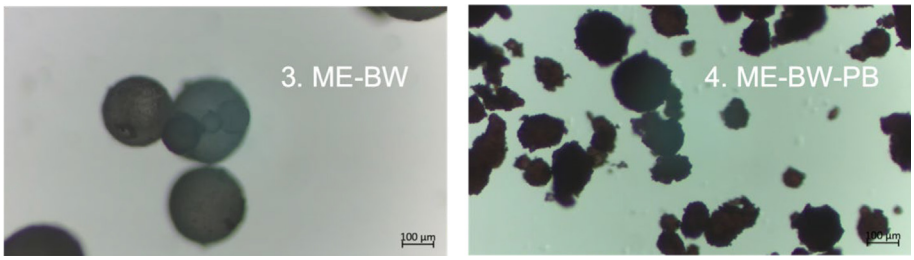

Fig. 1. Microscopic observations of particles generated by melt emulsification processes for Formulations 3. ME-BW (pure Beeswax) and 4. ME-BW-PB.

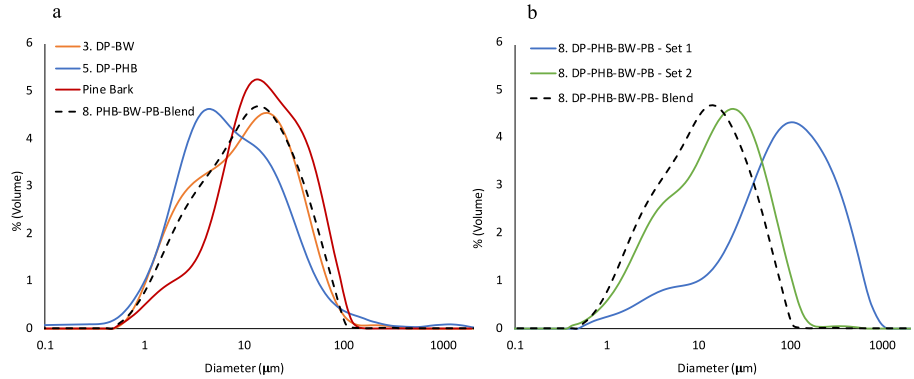

Fig. 2. (a) Particle size distribution of the pure components and of a blend of 3 components precipitated separately and mixed in the same ratio as Formulation 8. PHB-BW-PB. (b) Particle size distribution of Formulation 8. DP-BW-PW obtained according to the protocols for Set 1, Set 2, and mixed after precipitation.

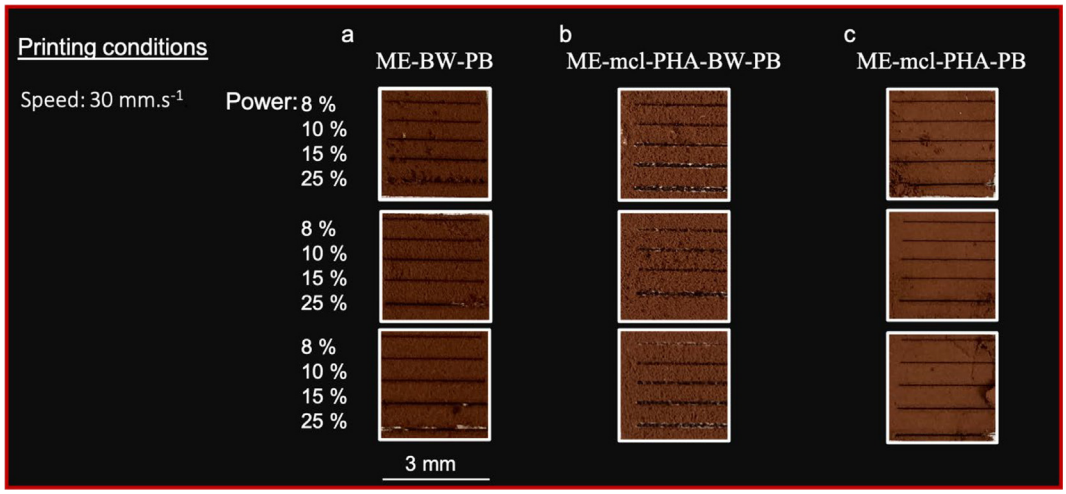

Fig. 3. Powder patterns obtained after laser sintering at different laser power for (a) beeswax/Pine bark; (b) mcl-PHA/BW/pine bark and (c) mcl-PHA/Pine Bark.

to be the most compact powder bed, also displays the highest printing resolution (Fig. 3c). Formulation 2 (ME-mcl-PHA-BW-PB) has the broadest particle size distribution. This was observed to significantly increase the porosity of powder bed due to poor spreadability, which in turn caused voids to be present between the particles. These are particularly apparent around the sintered (printed) shape due to the contraction of the powder. It is more evident when using a higher laser power, where the powder is not sintering anymore but rather fully melting (Fig. 3b). Interestingly, the powder from Formulation 4 (ME-BW-PB) appears to give better print quality than Formulation 2. ME-mcl-PHA-BW-PB, although it had the higher particle size. This may be explained by its lowest size distribution span.

These preliminary testing results confirm that the composite powders are printable using CO_2 laser sintering. Patterns with high resolution can be achieved for almost all the formulations tested at lower power (8% of the full power = 6 W). The next step will be to better control the particle size characteristics and carry out multi-layer prints for mechanical testing.

4. Conclusion

We have demonstrated proof-of-concept of processes enabling the production of composite biobased particles from biobased wax, lignocellulosic fillers, and two types of PHA. Two particle dissolution and precipitation methods including PHAs melt emulsifi-

cation and dissolution/precipitation in a deep eutectic solvent have been explored. The size of the particles obtained is comparable of those targeted for commercial powder-bed 3D printing, especially SLS printing. However, the process conditions significantly influence the size of the particles and the time in which the different components are in contact before the generation of the solid particles. In the case of dissolution/precipitation in deep eutectic solvent, it is proposed that this is the result of strong interactions between the components which are present during the dissolution phase. Preliminary SLS printing testing results have demonstrated that such powders are printable by SLS with high resolution and could be used for practical applications. However, the particle size characteristics of the powder strongly influence the quality of the printed shape. The next step will be the optimisation of both the SLS process and the particle properties.

Funding

Project SMARTPOP funded by H2020 - EU-MSCA-IF Grant number 893040.

MBIE grant number C04X1802 Bark biorefinery.

Use of artificial intelligence in scientific writing:

During the preparation of this work, the authors used OpenAI (2021), Chat GPT for spell and grammar checking.

CRediT authorship contribution statement

Claire Mayer-Laigle: Conceptualization, Investigation, Formal analysis, Writing – original draft, Writing – review & editing, Funding acquisition. **Christophe Collet:** Conceptualization, Investigation, Formal analysis, Writing – review & editing. **Yi Chen:** Conceptualization, Methodology, Investigation, Writing – review & editing. **Mark West:** Methodology, Investigation, Writing – review & editing. **Rob Whitton:** Methodology, Investigation, Writing – review & editing. **Marie-Joo Le Guen:** Conceptualization, Investigation, Formal analysis, Writing – original draft, Writing – review & editing, Funding acquisition.

Data availability

Data will be made available on request.

Declaration of Competing Interest

The authors declare the following financial interests/personal relationships which may be considered as potential competing interests: Claire Mayer-Laigle reports financial support was provided by European Commission. Marie-Joo Le Guen reports financial support was provided by Ministry of Business Innovation and Employment.

Acknowledgements

The authors thank Charlène Fabre and the PLANET facility run by the IATE joint research unit for providing valuable process experiment support in the preparation of lignocellulosic biomass powder.

Partnership

This research has been conducted as a part of the Scion-INRAE-U Montpellier - Institut Agro Associated International Laboratory BIOMATA.

References

[1] M. Saidani, E. Pan, H. Kim, Switching From Petroleum- to Bio-Based Plastics: Visualization Tools to Screen Sustainable Material Alternatives During the Design Process, (2020) http://doi.org/10.1115/DETC2020-22429.

[2] G. Coppola, M.T. Gaudio, C.G. Lopresto, V. Calabro, S. Curcio, S. Chakraborty, Bioplastic from Renewable Biomass: A Facile Solution for a Greener Environment, Earth Syst. Environ. 5 (2021) 231–251, https://doi.org/10.1007/s41748-021-00208-7.

[3] Q. Wang, Y. Xu, P. Xu, W. Yang, M. Chen, W. Dong, P. Ma, Crystallization of microbial polyhydroxyalkanoates: A review, Int. J. Biol. Macromol. 209 (2022) 330–343, https://doi.org/10.1016/j.ijbiomac.2022.04.018.

[4] A.L. Rivera-Briso, Á. Serrano-Aroca, Poly(3-Hydroxybutyrate-co-3-Hydroxyvalerate): Enhancement Strategies for Advanced Applications, Polymers (Basel) 10 (2018) 732, https://doi.org/10.3390/polym10070732.

[5] N. Ehman, A. Ponce De León, F. Felissia, M. Vallejos, M.C. Area, G. Chinga-Carrasco, Biocomposites of Polyhydroxyalkanoates and Lignocellulosic Components: A Focus on Biodegradation and 3D Printing, in: M. Kuddus, Roohi (Eds.) Bioplastics for Sustainable Development, Springer Singapore, Singapore, 2021, pp. 325-34510.1007/978-981-16-1823-9_13.

[6] C. Zarna, M.T. Opedal, A.T. Echtermeyer, G. Chinga-Carrasco, Reinforcement ability of lignocellulosic components in biocomposites and their 3D printed applications – A review, Compos. Part C: Open Access 6 (2021) 100171, https://doi.org/10.1016/j.jcomc.2021.100171.

[7] A. Dufresne, D. Dupeyre, M. Paillet, Lignocellulosic flour-reinforced poly (hydroxybutyrate-co-valerate) composites, J. Appl. Polym. Sci. 87 (2003) 1302–1315, https://doi.org/10.1002/app.11546.

[8] P. Cinelli, M. Seggiani, N. Mallegni, V. Gigante, A. Lazzeri, Processability and Degradability of PHA-Based Composites in Terrestrial Environments, Int. J. Mol. Sci. 20 (2019), https://doi.org/10.3390/ijms20020284.

[9] R.G. Craig, J.D. Eick, F.A. Peyton, Strength properties of waxes at various temperatures and their practical application, J. Dent. Res. 46 (1967) 300–305, https://doi.org/10.1177/00220345670460013101.

[10] S.P. Hlangothi, I. Krupa, V. Djoković, A.S. Luyt, Thermal and mechanical properties of cross-linked and uncross-linked linear low-density polyethylene–wax blends, Polym. Degrad. Stab. 79 (2003) 53–59, https://doi.org/10.1016/S0141-3910(02)00238-0.

[11] D. Robertson, A. van Reenen, H. Duveskog, A comprehensive investigation into the structure-property relationship of wax and how it influences the properties of hot melt adhesives, Int. J. Adhes. Adhes. 99 (2020) 102559, https://doi.org/10.1016/j.ijadhadh.2020.102559.

[12] J.P. Kalish, S. Ramalingam, H. Bao, D. Hall, O. Wamuo, S.L. Hsu, C.W. Paul, A. Eodice, Y.-G. Low, An analysis of the role of wax in hot melt adhesives, Int. J. Adhes. Adhes. 60 (2015) 63–68, https://doi.org/10.1016/j.ijadhadh.2015.03.008.

[13] V. Gigante, P. Cinelli, M.C. Righetti, M. Sandroni, G. Polacco, M. Seggiani, A. Lazzeri, On the Use of Biobased Waxes to Tune Thermal and Mechanical Properties of Polyhydroxyalkanoates-Bran Biocomposites, Polymers (Basel) 12 (2020), https://doi.org/10.3390/polym12112615.

[14] M.A. Vigil Fuentes, S. Thakur, F. Wu, M. Misra, S. Gregori, A.K. Mohanty, Study on the 3D printability of poly(3-hydroxybutyrate-co-3-hydroxyvalerate)/poly (lactic acid) blends with chain extender using fused filament fabrication, Sci. Reports, 10 (2020) 11804, http://doi.org/10.1038/s41598-020-68331-5.

[15] D. Tang, L. Hao, Y. Li, W. Xiong, T. Sun, X. Yan, Investigation of wax-based barite slurry and deposition for 3D printing landslide model, Compos. A Appl. Sci. Manuf. 108 (2018) 99–106, https://doi.org/10.1016/j.compositesa.2018.02.007.

[16] Y. Wang, J. Shen, M. Yan, X. Tian, Poly ether ether ketone and its composite powder prepared by thermally induced phase separation for high temperature selective laser sintering, Mater. Des. 201 (2021) 109510, https://doi.org/10.1016/j.matdes.2021.109510.

[17] M. Shahbazi, H. Jäger, Current Status in the Utilization of Biobased Polymers for 3D Printing Process: A Systematic Review of the Materials, Processes, and Challenges, ACS Appl. Bio Mater. 4 (2021) 325–369, https://doi.org/10.1021/acsabm.0c01379.

[18] W. Zhu, C. Yan, Y. Shi, S. Wen, J. Liu, Q. Wei, Y. Shi, A novel method based on selective laser sintering for preparing high-performance carbon fibres/polyamide12/epoxy ternary composites, Sci. Rep. 6 (2016) 33780, https://doi.org/10.1038/srep33780.

[19] M. Schmid, A. Amado, K. Wegener, Polymer powders for selective laser sintering (SLS), AIP Conf. Proc. 1664 (2015) 160009, https://doi.org/10.1063/1.4918516.

[20] X. Tardif, B. Pignon, N. Boyard, J.W.P. Schmelzer, V. Sobotka, D. Delaunay, C. Schick, Experimental study of crystallization of PolyEtherEtherKetone (PEEK) over a large temperature range using a nano-calorimeter, Polym. Test. 36 (2014) 10–19, https://doi.org/10.1016/j.polymertesting.2014.03.013.

[21] S. Berretta, K.E. Evans, O. Ghita, Processability of PEEK, a new polymer for High Temperature Laser Sintering (HT-LS), Eur. Polym. J. 68 (2015) 243–266, https://doi.org/10.1016/j.eurpolymj.2015.04.003.

[22] R. Ajdary, N. Kretzschmar, H. Baniasadi, J. Trifol, J.V. Seppälä, J. Partanen, O.J. Rojas, Selective Laser Sintering of Lignin-Based Composites, ACS Sustain. Chem. Eng. 9 (2021) 2727–2735, https://doi.org/10.1021/acssuschemeng.0c07996.

[23] A.I.B. Idriss, J. Li, Y. Wang, Y. Guo, E.A. Elfaki, S.A. Adam, Selective Laser Sintering (SLS) and Post-Processing of Prosopis Chilensis/Polyethersulfone Composite (PCPC), Materials 13 (2020), https://doi.org/10.3390/ma13133034.
[24] S. Fanselow, S.E. Emamjomeh, K.-E. Wirth, J. Schmidt, W. Peukert, Production of spherical wax and polyolefin microparticles by melt emulsification for additive manufacturing, Chem. Eng. Sci. 141 (2016) 282–292, https://doi.org/10.1016/j.ces.2015.11.019.
[25] Y. Yang, Z. Fang, X. Chen, W. Zhang, Y. Xie, Y. Chen, Z. Liu, W. Yuan, An Overview of Pickering Emulsions: Solid-Particle Materials, Classification, Morphology, and Applications, Front. Pharmacol. 8 (2017) 287.
[26] Z. Xiao, H. Cao, X. Jiang, X.Z. Kong, Pickering Emulsion Formation of Paraffin Wax in an Ethanol-Water Mixture Stabilized by Primary Polymer Particles and Wax Microspheres Thereof, Langmuir 34 (2018) 2282–2289, https://doi.org/10.1021/acs.langmuir.7b03802.
[27] J. Jiang, J. Cao, W. Wang, H. Shen, Preparation of a synergistically stabilized oil-in-water paraffin Pickering emulsion for potential application in wood treatment, Holzforschung 72 (2018) 489–497, https://doi.org/10.1515/hf-2017-0154.
[28] A. Paiva, R. Craveiro, I. Aroso, M. Martins, R.L. Reis, A.R.C. Duarte, Natural Deep Eutectic Solvents – Solvents for the 21st Century, ACS Sustain. Chem. Eng. 2 (2014) 1063–1071, https://doi.org/10.1021/sc500096j.
[29] C. Collet, A.A. Vaidya, M. Gaugler, M. West, G. Lloyd-Jones, Extrusion of PHA-containing bacterial biomass and the fate of endotoxins: A cost-reducing platform for applications in molding, coating and 3D printing, Mater. Today Commun. 33 (2022) 104162, https://doi.org/10.1016/j.mtcomm.2022.104162.
[30] R. Abbel, A.F. Greene, H. Quilter, J. Leveneur, R. Risani, M. Barbier, M. West, C. Collet, N.M. Kirby, M. Sorieul, Crystallization Behavior and Sensing Properties of Bio-Based Conductive Composite Materials, Adv. Eng. Mater. n/a (2022) 2200959, https://doi.org/10.1002/adem.202200959.
[31] K.R. Rajaonarivony, C. Mayer-Laigle, B. Piriou, X. Rouau, Comparative comminution efficiencies of rotary, stirred and vibrating ball-mills for the production of ultrafine biomass powders, Energy 227 (2021) 120508, https://doi.org/10.1016/j.energy.2021.120508.
[32] V. Agieienko, R. Buchner, Densities, Viscosities, and Electrical Conductivities of Pure Anhydrous Reline and Its Mixtures with Water in the Temperature Range (293.15 to 338.15) K, J. Chem. Eng. Data, 64 (2019) 4763–4774, http://doi.org/10.1021/acs.jced.9b00145.
[33] E. Dan Hirleman, Modeling of Multiple Scattering Effects in Fraunhofer Diffraction Particle Size Analysis, Part. Part. Syst. Char. 5 (1988) 57–65, https://doi.org/10.1002/ppsc.19880050202.
[34] S. Berretta, O.R. Ghita, K.E. Evans, A. Anderson, C. Newman, Size, shape and flow of powders for use in Selective Laser Sintering (SLS), 2013,
[35] Y. Yu, M. Jiang, S. Wang, Y. Guo, T. Jiang, W. Zeng, Y. Zhuang, Impact of Particle Size on Performance of Selective Laser Sintering Walnut Shell/Co-PES Powder, Materials 14 (2021), https://doi.org/10.3390/ma14020448.
[36] M. Jablonský, A. Škulcová, J. Šima, Use of Deep Eutectic Solvents in Polymer Chemistry–A Review, Molecules 24 (2019), https://doi.org/10.3390/molecules24213978.